Available online at www.sciencedirect.com

ScienceDirect

journal homepage: www.elsevier.com/locate/he

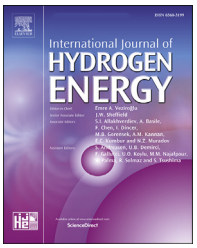

Multi-objective optimization and exergoeconomic analysis of a multi-generation system based on biogas-steam reforming☆

Jinghan He [a], *Ninghui Han* [a], *Mingchao Xia* [a], *Tianyi Sun* [b,c,**], *Hadi Ghaebi* [d,*]

[a] School of Electrical Engineering, Beijing Jiaotong University, Beijing 100044, China
[b] School of Automation Engineering, Northeast Electric Power University, Jilin, China
[c] School of Information Engineering, Nanchang University, Nanchang, China
[d] Department of Mechanical Engineering, University of Mohaghegh Ardabili, P.O. Box 179, Ardabil, Iran

HIGHLIGHTS

- Proposing a tri-generation system for power, cooling and hydrogen production.
- Proposing biogas-steam reforming as base system.
- Application of power generation and refrigeration systems.
- Using R236fa refrigerant in subsystems because it is environmentally friendly.
- Applying single-objective and multi-objective optimization methods.

ARTICLE INFO

Article history:
Received 21 July 2022
Received in revised form
4 December 2022
Accepted 7 December 2022
Available online xxx

Keywords:
Biogas
Kalina cycle
Hydrogen
Ejector
Exergy analysis

ABSTRACT

In the current work, a new design of a multi-generation integrated energy system powered by biogas energy is proposed, assessed, and optimized. To scrutinize the workability of the offered system, energy, exergy, exergo-economic, and economic investigations have been applied as robust tools to the evaluation of the system. Moreover, to boost the rate of hydrogen production rate, the steam reforming method and purification process are integrated into the systems. It is found that the designed multi-generation integrated energy system is able to generate 108.7 kW, 888.7 kW, and 703.3 kg/h, power, cooling load, and hydrogen, sequentially. Besides, it is determined that the energy and exergy efficiencies of the system are about 31.51% and 31.14%, sequentially. Furthermore, a comprehensive parametric evaluation is employed to appraise the influences of key variables on the operation of the system and relying on its achieved outcomes, two different optimization styles are established. From the optimization outcomes, it is remarked that in the multi-objective optimization mode, a TCOP of 16.23 S/GJ and a net power of 158.21 KW, are achievable.

☆ Note: Beijing Jiaotong University and Northeast Electric Power University are the co-first affiliation of this paper.

* *Corresponding author.*
** *Corresponding author.*
E-mail addresses: tianyisun2022@163.com (T. Sun), hghaebi@uma.ac.ir (H. Ghaebi).

https://doi.org/10.1016/j.ijhydene.2022.12.093
0360-3199/

Please cite this article as: He J et al., Multi-objective optimization and exergoeconomic analysis of a multi-generation system based on biogas-steam reforming, International Journal of Hydrogen Energy, https://doi.org/10.1016/j.ijhydene.2022.12.093

Nomenclature

Symbols

A	Area
c	Cost per unit of exergy, $/GJ
$\dot{c}$	Cost rate, $/year
ex	Specific exergy, kJ/kg
$\dot{E}X$	Exergy rate, kW
h	Enthalpy, $kJ.kg^{-1}$
I_r	Interest rate, %
$\dot{m}$	Mass flow rate, kg/s
P	Pressure, bar
Q	Heat
r	Relative cost difference
s	Entropy, $kJ.kg^{-1}.K^{-1}$
T	Temperature, K
U	Coefficient of heat transfer, kW/m^2K
$\dot{w}$	Power, kW
y	Concentration of ammonia
Z	Capital investment cost, $

Acronyms

CRF	Factor of capital recovery
CHP	Combined heat and power
EES	Engineering equation solver
FC	Fixed cost
GA	Genetic Algorithm
LHV	Low heating value
NPV	Net present value
PP	Payback period
PEME	Proton exchange membrane electrolyzer
TCOP	Total cost of products

Subscripts and superscripts

0	Reference condition
bio	Biogas
CP	Compressor
D	Destruction
env	Environmental
en	Energy
EVA	Evaporator
fu	Fuel
pr	Product
Reac	Reactor
tot	Total

Greek symbols

η	Efficiency
φ	Maintenance factor

Introduction

It is no secret that there is a tight and direct relationship between fossil fuel consumption, air pollution, and greenhouse gas emissions [1,2]. Exploring more green options to respond to unbridled demand for energy and other needs for human beings such as drinking water and cooling/heating loads has always been an alluring challenge for experts and scholars [3–5]. Energy systems include a wide range of plants from traditional energy systems that have generated just heat and power (CHP) to the most recent ones (multi-generation energy systems) that are designed to synthesize more than three outputs. Improving efficiency, decreasing the final product cost and negative environmental effects are some most vital criteria that always have been followed by designers [6,7]. In recent years, different ways of producing hydrogen as a clean energy carrier have captured the attention of researchers [8,9]. Correspondingly, the freshwater generation in the multi-generation systems was observed in different thermal and membrane methods [10,11]. Innovative energy systems are considered the most recent plants that are designed to use the maximum potential of inlet energy to generate useful products such as heating or heating loads, desalinated water, hydrogen, and other chemicals. For an instance, Li et al. [12] evaluated a renewable-based tri-generation system to produce electricity, cooling load, and hydrogen, simultaneously. In the proposed system a common proton exchange membrane electrolyzer (PEME) has been considered to synthesize the hydrogen. Results showed that the net generated electricity, cooling load and synthesized hydrogen reached 451.8 kW, 297.8 kW, and 2.274 kg/h. You et al. [13] designed and evaluated a solar-driven tri-generation plant for power, heating, and cooling load generation. They utilized supercritical carbon dioxide for power generation, a lithium bromide absorption system for cooling load provision, and thermal energy extraction from all corners of the proposed plant for heating load provision. It was found that the effectiveness of the energy exchanger and the pressure ratio of the recombination cycle play the most critical roles in the system concerning the best performance of the system. Colakoglu and Durmayaz [14] developed a multi-generation plant driven by solar energy to produce hydrogen, cooling, power, and domestic hot water. Two domestic water heaters, a single-effect absorption system, and a thermal energy storage unit were applied in the mentioned plant. After evaluating the system via thermodynamic laws, the determination of optimal operation conditions was carried out by multi-objective optimization and the hydrogen production rate reached 22.48 kg/h. The thermoeconomic assessment and the multi-criteria optimization were done on a solar-driven hydrogen production energy-based plant by Cao et al. [15]. In the proposed system the generated hydrogen via a solar-powered energy system was injected into a biomass gasification-solid oxide fuel cell (SOFC) to improve the final synthesize hydrogen. The findings unfold that the proposed system has a lower environmental negative impact (related to greenhouse gas emission) and higher output electricity in comparison to the conventional plant. Ghaebi et al. [9] checked an original configuration of a SOFC/gas turbine incorporated cycle plant with a biogas reforming cycle aiming to cogeneration the generation of hydrogen and electric

Please cite this article as: He J et al., Multi-objective optimization and exergoeconomic analysis of a multi-generation system based on biogas-steam reforming, International Journal of Hydrogen Energy, https://doi.org/10.1016/j.ijhydene.2022.12.093

power. Parametric investigations had been studied for the effect of different parameters on the electricity, energetic and exergetic proficiencies, rate of destroyed exergy, and the total product cost rate of the whole system. The results depicted that the energetic and exergetic proficiencies of the proffered combined system had raised compared to the SOFC/gas turbine system by approximately 23% and 28%, individually. The electricity and hydrogen rates were attained at approximately 2726 kW plus 0.075 kg/s, individually. Hashemian and Noorpoor [16] investigated and optimized a novel geothermal-biomass-powered multi-generation system with green hydrogen, cooling, power, and freshwater generation from techno-economic-environmental aspects. As they reported the recommended plant produced 88.1 kg/h of hydrogen and 23.3 m^3/h of freshwaters. Moreover, optimal exergetic efficiency and total product cost rate were attained at about 17.3% and 1.6 $/s. Biogas was employed as the power source to drive an innovative cogeneration energy system developed by Ghaebi et al. [17]. In this system, an organic Rankine cycle was considered to generate power, and a steam reforming method was employed to reform biogas and turn it into hydrogen. The proposed system was modeled and then the objective functions were optimized to determine the best operation conditions. Reportedly, in the optimum circumstance, the proposed system can generate 15.9 kW of electricity and 0.02529 kg/s of hydrogen. Besides, the optimal energy and exergy efficiencies were reported at 45.63% and 74.89% respectively. Situmorang et al. [18] tested the biogas direct chemical looping process into a small-scale energy system to generate power and simulated it in Aspen Plus™ software. The findings demonstrated that the proposed chemical looping-based system has higher efficiency in comparison to the conventional biomass firing CHP systems. In another research [19], the biogas employed to drive a basic and modified energy system, and the obtained results were compared concerning thermodynamic aspects of compared systems. It was found that by increasing the air compressor pressure ratio and steam turbine's inlet pressure the efficiencies of both systems improve. Moreover, based on the thermoeconomic evaluation, it was observed that the cost of the final product can be minimized if the inlet temperature of the gas turbine enhances. Minutillo et al. [20] scrutinized two poly-generation plants with focusing on green hydrogen synthesis from biogas. The first one utilized the biogas-steam reforming method to convert biogas to hydrogen, while the second one applied an auto-thermal reforming process to generate hydrogen. Based on the findings, the auto thermal reforming-based plant works more efficiently from energy and exergy standpoints. However, the biogas-steam reforming-based plant has better performance in the co-production of heat and hydrogen compared to other plants.

As reviewed in the literature, applying biogas as the main fuel to run innovative energy systems that include methane and carbon dioxide is an alluring idea that this work tries to investigate for the first time. Moreover, hydrogen synthesizing during the production process in such a system is another novelty of this work. The last significant aspect of the suggested system is related to arranging three different evaporators with operation ranges between upper and under zero temperatures. In the current study, a multi-generation plant for the simultaneous generation of power, cooling, fresh water, and hydrogen was developed. The remarkable innovations of the current investigation are as follows:

- Designing a carefully integrated multi-generation energy system driven by the biogas-steam reforming cycle which can be operated in wider temperature and pressure ranges and performs with higher efficiency compared to existing ones.
- Employing R236fa as an environmentally-friendly working fluid can boost the efficiency of cooling load production.
- Conducting comprehensive parametric studies from thermodynamic, thermoeconomic, and economic standpoints. Also, the net present value and payback period indicators have been calculated by considering all effective factors in the administrative prices of the suggested system.
- Implementing the single-objective and multi-objective optimizations and proving the Pareto frontier to argue and select the best trade-off operating point from techno-economic aspects.

System description

The illustration of the proposed system has been depicted in Fig. 1. The mentioned energy system has been designed for the simultaneous production of power, cooling, and hydrogen in an integrated system. The system includes two main subsystems: The Kalina cycle with the Rankine cycle, and the organic flash cycle with the ejector.

The exiting gaseous stream from the water pre-heater (stream 10) has remarkable thermodynamic features that can be applied to drive thermodynamic-based energy systems. To this end, two different sub-systems have been designed to utilize this heating capacity. The first sub-system runs based on the Kalina cycle, while the second one has been designed to work under the organic flash cycle's rules. Stream 10 passes through vapor generator 1 (VG1) and injects the heat into steam 16, which heats it. Stream 16, with a high temperature, enters separator 1 (SEP1) and is split into saturated vapor and saturated liquid. Then, the saturated vapor goes to turbine 1 (TUR1) and makes shaft power, and, after losing its high thermodynamic properties, enters mixer 2 (Mix2). The significant point that must be highlighted here about the second stream is that stream 19 includes saturated liquid with high thermodynamic properties that have enough potential to drive another sub-system. To this end, a combined Rankine and vapor compression refrigeration cycle has been designed to generate power and cooling load. R236fa refrigerant is employed as working fluid in the subsystems due to its environmental friendliness and also producing more cooling load than other refrigerants. Stream 32 passes through vapor generator 2 (VG2) in the mentioned cycle and becomes superheated. After passing through, turbine 2 (TUR2) generates shaft power. On the other hand, the exiting flow from evaporator 1 (EVA1) enters compressor 1 (CP1) and is pressurized. Then, the high-pressure flow (stream 36) mixes with stream 28 and goes to the thermoelectric generator (TEG2). The main reasons for considering this element (TEG) in the system are power generation and reducing heat loss in the condenser.

Please cite this article as: He J et al., Multi-objective optimization and exergoeconomic analysis of a multi-generation system based on biogas-steam reforming, International Journal of Hydrogen Energy, https://doi.org/10.1016/j.ijhydene.2022.12.093

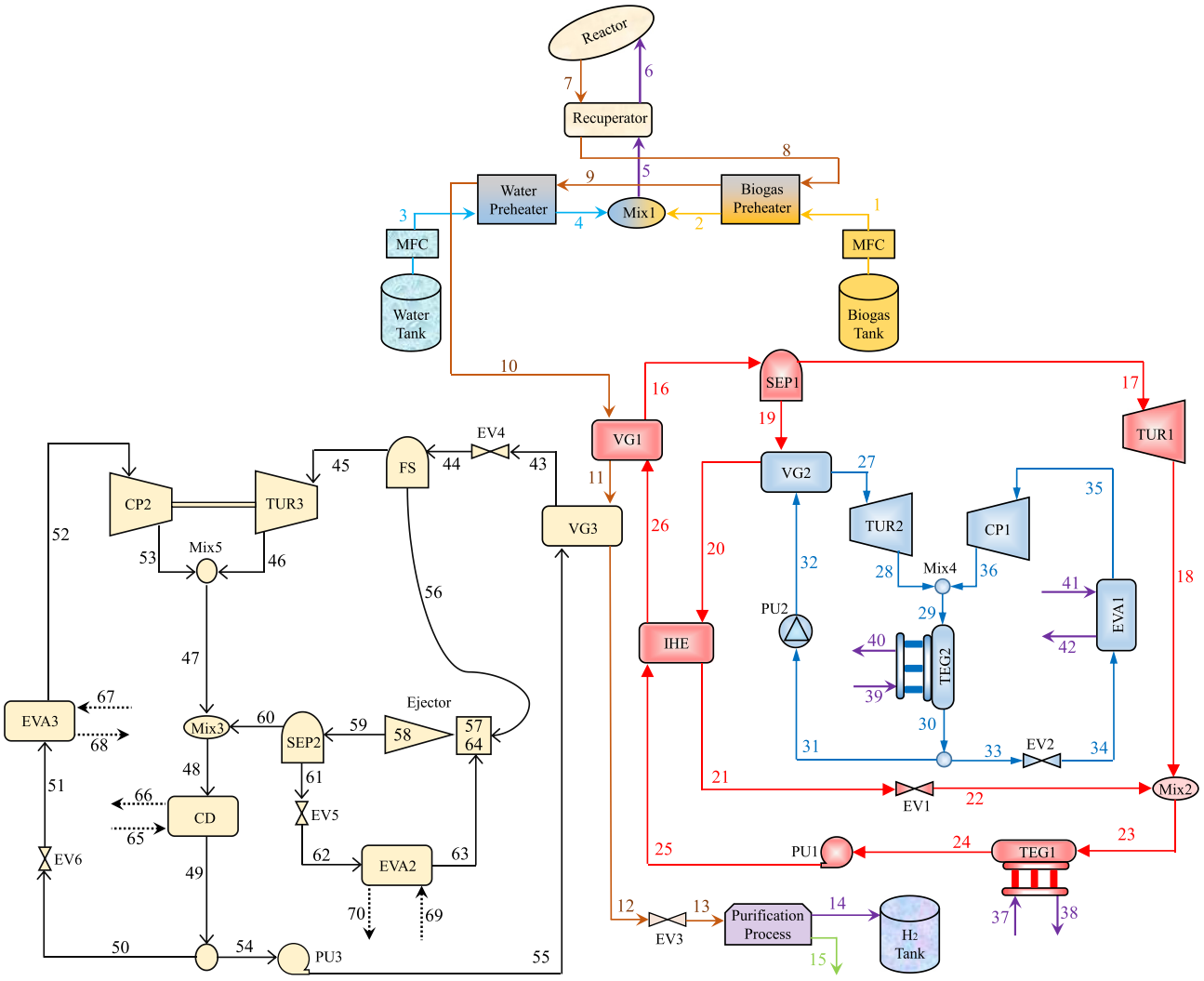

Fig. 1 – The illustration of the proposed energy system for simultaneous production of power, cooling, freshwater, and hydrogen. (VG: Vapor Generator, SEP: Separator, TUR: Turbine, Mix: Mixer, EVA: Evaporator, CP: Compressor, TEG: Thermoelectric Generator, PU: Pump, EV: Expansion Valve, IHE: Heat Exchanger, FS: Flashing Separator, CD: Condenser).

After generating power in TEG, stream 30 is divided into two streams (31 and 33). Stream 31 passes through pump 2 (PU2) and reaches stream 33's thermodynamic properties, while stream 33 goes to expansion valve 2 (EV2) and then enters evaporator 1 (EV1). To boost the input temperature of vapor generator 1 (VG1), stream 19 passes through vapor generator 2 (VG2). Then, stream 21 exits the heat exchanger (IHE) and goes to expansion valve 1 (EV1). The outlet stream of expansion valve 1 (stream 22) mixes with stream 18, and the mixed fluid goes to thermoelectric generator 1 to generate the shaft power. Finally, in the last stage of the Kalina cycle-based sub-system, the low-temperature fluid (stream 24) flows into pump 1 (PU1) and the heat exchanger (IHE) to adsorb heat and enter vapor generator 1 (VG1). On the other hand, the gaseous outlet stream of VG1 (stream 11) has suitable thermodynamic features to trigger another sub-system. In this regard, an integrated sub-system was designed that consists of three different elements (organic flash cycle, ejector refrigeration, and compression refrigeration cycle). Stream 43 in the form of saturated liquid goes to expansion valve 4 (EV4) and, after passing this element, turns into the two-phase flow. Then, the two-phase flow enters the flashing separator (FS) to be divided into two different flows (liquid and steam). The separated steam goes to turbine 3 (TUR3) to generate the shaft power. Next, the turbine's outlet stream (stream 46) enters mixer 5 (Mix5). Stream 52 from evaporator 3 (EV3) is compressed by compressor 2 (CP2) and then enters Mix5. On the other hand, the saturated liquid exits from FS as the primary flow, and saturated vapor exits from EV2 as the secondary flow, going to the ejector. The outlet flow of the ejector is a two-phase stream, and due to this feature, it is sent to the separator 2 (SEP2) to be divided into two streams (liquid and vapor). The separated saturated liquid goes to the expansion valve (EV). It then is conducted into EV2, while another part (separated saturated vapor) combines with stream 47 in Mix3, which, after passing through the condenser (CD), reaches the properties of saturated liquid and then separates into two streams (streams 50 and 54). Stream 54 passes through PU3 and

Please cite this article as: He J et al., Multi-objective optimization and exergoeconomic analysis of a multi-generation system based on biogas-steam reforming, International Journal of Hydrogen Energy, https://doi.org/10.1016/j.ijhydene.2022.12.093

reaches the pressure of state 55, while stream 50 passes through EV6 and goes to EV3 to complete the sub-system designed based on the organic flash cycle.

System modeling

The thermodynamic (energy and exergy theories) and thermoeconomic performances of the proposed system are assessed using a mathematical model through Engineering Equation Solver (EES) software [21] developed in this section. To interpret the simulation several assumptions and input data are held as follows in Table 1.

Table 1 – Assumptions and input data for system modeling.

Parameter	Value	Reference
Environmental temperature, T_0 (K)	293.15	[22]
Environmental pressure, P_0 (*bar*)	1.01	[22]
Reforming cycle		
Biogas temperature, T_{Bio} (K)	293.15	[23]
Biogas pressure, P_{Bio} (*bar*)	6.895	[23]
Reactor pressure, P_{Reac} (*bar*)	1.5	[23]
Reactor temperature, T_{Reac} (K)	967.15	[23]
Biogas preheated temperature difference, ΔT_{Biogas} (K)	44	[23]
Water tank outlet temperature, T_3 (K)	293.15	[23]
Recuperator efficiency, ε_{rec} (%)	80	[23]
Steam to carbon molar ratio, S_c	1.5	[23]
Carbon dioxide to methane molar ratio, C_m	0.5	[23]
Subsystems		
Evaporators temperature, T_{EVA} (K)	275	[24]
Ammonia concentration of the basic solution, Y_B (%)	65	[22]
Separator 1 pressure, P_{16} (bar)	30	[22]
TEGs outlet temperature, $T_{24}; T_{30}$ (K)	303	[22]
Vapor generators terminal temperature difference , $\Delta T_{TTD,VG}$ (K)	10	–
Flashing separator temperature, T_{44} (K)	363.15	[25]
Condenser terminal temperature difference , $\Delta T_{TTD,CD}$ (K)	5	–
Pumps isentropic efficiency, $\eta_{is,PU}$ (–)	0.9	[22]
Turbines isentropic efficiency, $\eta_{is,TUR}$ (–)	0.85	[26]
Compressors isentropic efficiency, $\eta_{is,CP}$ (–)	0.85	[27]
Motive nozzle efficiency of ejector, η_{mn} (–)	0.9	[26]
Suction nozzle efficiency of ejector, η_{sn} (–)	0.9	[26]
Mixer efficiency of ejector, η_m (–)	0.85	[26]
Diffuser efficiency of ejector, η_d (–)	0.88	[26]
Cooling water temperature, $T_{37}; T_{39}; T_{67}$ (K)	293.15	[22]
Economic parameters		
Annual operating hours, N (*h*)	7446	[22]
Maintenance factor, φ_r	1.06	[22]
Annual interest rate, I_r (%)	12	[22]
Lifetime of the Components, n_r (years)	20	[22]
Biogas unit cost, c_{Bio} ($/GJ)	7.36	[28]

This section is subdivided into three divisions, including methodologies for inquiries of energy, exergy, and economics of the proposed system.

Energy analysis

Confirming the above presumptions, the mass and energy balance relations are applied for elements based on the first and second laws of thermodynamics [29].

$$\sum \dot{m}_{inlet} = \sum \dot{m}_{outlet} \tag{1}$$

$$\sum \dot{Q} - \sum \dot{W} = \sum \dot{m}_{outlet}\dot{h}_{outlet} - \sum \dot{m}_{inlet}\dot{h}_{inlet} \tag{2}$$

where, $\dot{m}, \dot{W}$, and $\dot{Q}$ signify mass flow rate, power, and rate of heat transfer of the control volume, sequentially. The energy analyses for all control volumes are accompanied by steady-state situations. Also, flow crossed the expansion valves as isenthalpic [30,31].

The details of useful equations applied for the ejector modeling are presented in Table 2.

Therefore, the performance of the system can be evaluated by the energy efficiency of the system, shown as:

$$\eta_{en} = \frac{\dot{W}_{net} + \dot{Q}_{EVA1} + \dot{Q}_{EVA2} + \dot{Q}_{EVA3} + \dot{m}_{14}LHV_{H_2}}{\dot{Q}_{Reac} + \dot{m}_1 LHV_{biogas}} \times 100 \tag{3}$$

Here

$$\dot{W}_{net} = \dot{W}_{TUR1} + \dot{W}_{TUR2} + \dot{W}_{TUR3} + \dot{W}_{TEG1} + \dot{W}_{TEG2} - \dot{W}_{PU1} - \dot{W}_{PU2} - \dot{W}_{PU3} - \dot{W}_{CP1} - \dot{W}_{CP2} \tag{4}$$

Exergy analysis

Exergy interpretation is recognized as an appropriate tool to assess the performance of an energy production system. The exergy balance based on the Fuel-Product method can be written for the i element of a system as follows:

$$\dot{E}x_{fu,i} = \dot{E}x_{pr,i} + \dot{E}x_{D,i} \tag{5}$$

Here, $\dot{E}x$ represents the exergy rate, and the indexes fu, pr, and D indicate fuel, product, and destruction, respectively. To provide the exergy analysis, all stream exergy ought to be calculated, if we neglect the kinetic and potential exergies of the system, exergy balances are formulated as underneath [2]:

$$\dot{E}x_{tot,i} = \dot{E}x_{ph,i} + \dot{E}x_{ch,i} \tag{6}$$

$$\dot{E}x_{ph,i} = \dot{m}(h_i - h_0 - T_0(s_i - s_0)) \tag{7}$$

$$\dot{E}x_{ch,i} = \dot{m}\left(\sum_i y_i \overline{ex}_i^{ch,O} + \overline{R}T_O \sum_i y_i ln y_i\right)_k \tag{8}$$

Indexes ph and ch signify the physical and chemical. 0 signifies the reference point. Also, h and s are specific enthalpy and entropy of the stream, respectively, while T_0 and P_0 are at reference states of temperature and pressure. Also, $\overline{ex}_i^{ch,O}$ is the standard chemical exergy of the mixture.

Please cite this article as: He J et al., Multi-objective optimization and exergoeconomic analysis of a multi-generation system based on biogas-steam reforming, International Journal of Hydrogen Energy, https://doi.org/10.1016/j.ijhydene.2022.12.093

Table 2 – Ejector modeling equations [32–34].

	Equation	Equation number
Ejector mass entrainment ratio	$\mu = \frac{\dot{m}_{63}}{\dot{m}_{56}}$	(3)
Isentropic efficiency of motive nozzle	$\eta_{mn} = \frac{h_{56} - h_{57}}{h_{56} - h_{57,is}}$	(4)
Energy balance between the nozzle and primary flow sections	$h_{56} - h_{57} = \frac{1}{2}C_{57}^2$	(5)
Momentum balance for mixing section	$C_{58} = \sqrt{\eta_m}\left(\frac{C_{57}}{1+\mu}\right)$	(6)
Ejector's energy balance	$h_{58} = \frac{h_{56} + \mu h_{63}}{1+\mu} - \frac{C_{58}^2}{2}$	(7)
Energy balance between mixing and outlet section	$h_{59} = h_{58} + \frac{1}{2}C_{58}^2$	(8)
Diffuser efficiency	$\eta_d = \frac{h_{59,is} - h_{58}}{h_{59} - h_{58}}$	(9)
New ejector mass entrainment ratio	$\mu_{new} = \sqrt{\frac{\eta_{mn}\eta_m\eta_d(h_{56} - h_{57,is})}{h_{59,is} - h_{58}}} - 1$	(10)

To assess system proficiency from the second law prospect, exergy efficiency is applied. For the suggested system the exergy efficiency is represented as:

$$\eta_{ex} = \frac{\dot{W}_{net} + \dot{E}x_{42} + \dot{E}x_{70} + \dot{E}x_{68} + \dot{E}x_{14}}{\dot{E}x_{Fu}^{Reac} + \dot{E}x_1} \times 100 \quad (9)$$

Economic analysis

Thermo-economic approach

The thermo-economic inquiry accommodates both thermodynamic and economic aspects till values the system's total product cost, holding capital and investment expenditures, operating and maintenance expenses, and additional relevant expenses. The following equations are employed to turn these estimated expenses toward the rates of cost. $\dot{Z}_k$ and Z_{total} hold the cost of capital investment and the summation of the costs of the investment and operation and maintenance, respectively, and are computed by Ref. [35]:

$$\dot{Z}_k = \frac{Z_k \times \varphi_r \times CRF}{N} \quad (10)$$

$$Z_{total} = Z_{investment} + Z_{O\&M} = \varphi_r \times Z_{investment} \quad (11)$$

where, φ_r and N stand the factor of maintenance and the plant's yearly work hours, considered to be 1.06 and 7446 h, and CRF is the factor of capital recovery:

$$CRF = \frac{I_r(I_r+1)^{n_r}}{(1+I_r)^{n_r} - 1} \quad (12)$$

I_r and n_r denote the rate of interest and the plant lifetime, fixed to be 0.12 and 20 years in the current study [36]. Therefore, the total cost of the products can be determined as:

$$TCOP = \frac{CRF \times Z_{total} + (\dot{C}_{Bio}) \times N}{N \times (\dot{W}_{net} + \dot{E}x_{42} + \dot{E}x_{70} + \dot{E}x_{68} + \dot{E}x_{14})} \quad (13)$$

Relying on the description of logarithmic mean temperature difference ($\Delta T_{LMTD,k}$) and the overall coefficient of heat transfer (U_k), the area of the heat transfer may be calculated as:

$$A_k = \frac{\dot{Q}_k}{U_k \Delta T_{LMTD,k}} \quad (14)$$

$$\Delta T_{LMTD} = \frac{\Delta T_A - \Delta T_B}{ln\frac{\Delta T_A}{\Delta T_B}} \quad (15)$$

The elements' cost balance relations for each component of the system are listed in Table 3.

Net present value (NPV) approach

The NPV method indicates the value of the investment regarding future profits and the possible discount in the cash flows. These variables can be formulated as:

$$NPV = -FC + \sum_{i=1}^{n}(ANS \times IF_i \times RDF_i) \quad (16)$$

Here, i depicts the period based on year, FC denotes the fixed cost, ANS shows the annual net saving money, and R represents the inflation rate.

Table 3 – Component cost relations.

Component	Cost function ($)	Reference
Biogas preheater	$2143 \times (A_{Bio-Pre})^{0.514}$	[37]
Compressors	$10167.5 \times (\dot{W}_{COMP})^{0.46}$	[38]
Condenser	$516.62 \times (A_{CD})^{0.6}$	[28]
Ejector	$13.5 \times P_{59}{}^{-0.75} \times (T_{56}/P_{56})^{0.05}$	[28]
Evaporators	$276 \times (A_{EVA})^{0.88}$	[28]
Expansion Valves	$114.5 \times \dot{m}$	[28]
IHE	$130 \times (A_{IHE}/0.093)^{0.78}$	[35]
Pumps	$900 \times (\dot{W}_{PU}/300)^{0.25}$	[25]
Reactor	$283 \times (\dot{Q}_{Reac})$	[37]
Recuperator	$2143 \times (A_{Bio-Rec})^{0.514}$	[37]
TEGs	$1000 \times \dot{W}_{TEG}$	[39]
Turbines	$4405 \times (\dot{W}_{TUR})^{0.71}$	[40]
Vapor Generators	$130 \times (A_{VG}/0.093)^{0.78}$	[16]
Water preheater	$2143 \times (A_{W-Pre})^{0.514}$	[37]

Please cite this article as: He J et al., Multi-objective optimization and exergoeconomic analysis of a multi-generation system based on biogas-steam reforming, International Journal of Hydrogen Energy, https://doi.org/10.1016/j.ijhydene.2022.12.093

Table 4 – The formulation of the fixed cost.

Variable	Equation
Direct costs (DC)	(Onsite costs)+(Offsite costs)
Onsite costs	
Investment cost	$Z_{investment}$
Purchased-equipment installation	$0.33 \times Z_{investment}$
Piping	$0.35 \times Z_{investment}$
Electrical equipment and materials	$0.13 \times Z_{investment}$
Offsite costs	
Land	$0.05 \times Z_{investment}$
Civil, structural, and architectural work	$0.21 \times Z_{investment}$
Service facilities	$0.35 \times Z_{investment}$
Indirect costs (IC)	
Engineering and supervision	$0.08 \times DC$
Construction costs including contractor's profit	$0.15 \times DC$
Contingencies	$0.15 \times (1.23 \times DC)$

$$IF_i = \left(1 + \frac{R}{100}\right)^{-i} \quad (17)$$

$$RDF_i = \left(1 + \frac{i_r}{100}\right)^{-i} \quad (18)$$

Also,

$$FC = DC + IC \quad (19)$$

where DC and IC are the direct and indirect costs presented in Table 4.

According to,

$$ANS = AI - OC \quad (20)$$

$$OC = 0.06 \times FC \quad (21)$$

Here, AI and OC are the annual income of the system and its operating cost.

The payback period of the projected system is equal to the time that the initial investment can recover and the system starts to generate income. Initially, the value of the NPV is negative, when this variable gives a positive amount, it can be expressed that the system witnesses revenue. Simply put, the payback period (PP) of the system, when the NPV is positive for the first time, this variable is calculated as follows:

$$PP = \frac{FC}{ANS} \quad (22)$$

Table 5 – Decision variables and their analytical ranges.

Parameter	Range
Steam to carbon molar ratio, S_c	$1 \le S_c \le 3$
Carbon dioxide to methane molar ratio, C_m	$0.1 \le C_m \le 0.7$
Reactor pressure, P_{Reac} (bar)	$1 \le P_{Reac} \le 3$
Reactor temperature, T_{Reac} (K)	$950 \le T_{Reac} \le 1200$
Evaporator temperature, T_{EVA}(K)	$268 \le T_{EVA} \le 283$
Environmental temperature, T_0(K)	$285 \le T_0 \le 300$

Optimization

In the current work, the Genetic Algorithm (GA) has been applied by weighing multi-chief objective functions, specifically net power and TCOP. In the single-objective optimization case, the principal purpose is to maximize net power or minimize the TCOP, individually relying on determined decision parameters. Concerning the multi-objective optimization case, every function has weighed independently and outcomes are combined collectively [41,42]. Respected to this approach, a Multi-Objective Function (MOF) is set and the aim is to maximize the net power criteria function and to minimize the TCOP concurrently. For the suggested system, the equations are set below [43]:

$$MOF = w_1 \times \dot{W}_{net} + (1 - w_2 \times TCOP) \quad (23)$$

$$w_1 + w_2 = 1 \quad (24)$$

$$0 \le w_1 \; ; \; w_2 \le 1 \quad (25)$$

Table 5 represents the decision variables and their analytical ranges for the optimization procedure.

Results and discussions

Before giving the results, a model validation to show the precision of the modeling results would be helpful.

Model validation

This section proffers a comparison between the achieved results from the modeling of the proposed system and the related previously published inquiries. This action is carried out to clarify the truth and the verification of results. In this regard, some sub-systems of the proposed energy system are compared with similar research that had been published, recently. Each verification is supporting similar internal and external situations. In Fig. 2, the model validation between the energy efficiency of the organic flash cycle in the present study

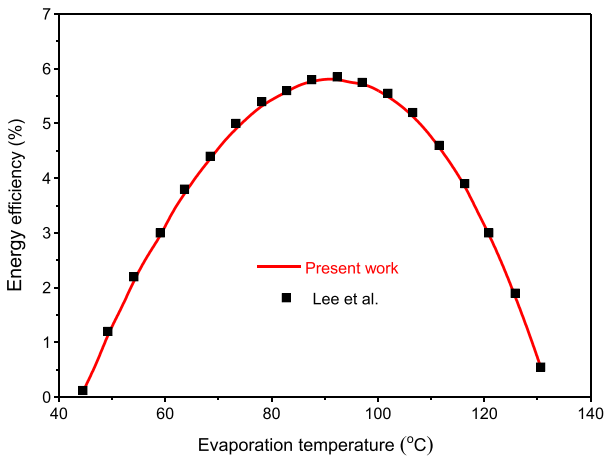

Fig. 2 – Results comparison of the organic flash cycle between the present study and ref [44].

Table 6 – Model validation between the present study with ref [45].

Parameter	Present study	Ref	Relative error (%)
S_c	2	2	0
Reaction pressure (bar)	1.5	1.5	0
Reaction temperature (K)	967.15	967.15	0
Product H_2 molar fraction	0.60837	0.6039	0.73
Product CH_4 molar fraction	0.01772	0.01849	4.1
Product CO molar fraction	0.1491	0.1375	7.7
Product CO_2 molar fraction	0.04027	0.04356	7.5
Product H_2O molar fraction	0.1845	0.1835	0.5

Table 7 – The validation of this study for the Kalina cycle.

Parameters	P = 3 MPa		P = 2.5 MPa		P = 2 MPa	
	Ref. [46]	PS	Ref. [46]	PS	Ref. [46]	PS
Maximum η_{en} (%)	10.20	10.28	9.5	9.55	9.02	9.18
Optimum Y_B (%)	75.4	74.9	68.5	68.0	60.9	59.6

with research by Lee et al. [44] by evaporation temperature variation is presented. Moreover, R123 has been employed as an operating fluid same as ref [44]. As can be seen in the figure, modeling results are in good agreement with ref [44].

Also, Table 6 proves a comparison between the obtained results of the current study and the reported results by Wegeng et al. [45]. As can be seen in Table 8, the influence of the reaction pressure and temperature plus the molar fraction product of hydrogen, methane, carbon monoxide, carbon dioxide, and water have been compared. It is crystal clear that, based on the relative errors, the modeling results of the present work are in a good deal with the related results in Ref. [45].

In Table 7, the Kalina cycle model verification between the present study under three different pressure and ref [46] is given. As may be seen in the stated table, maximum energy efficiency and optimum Ammonia concentration of the basic solution results verify the accuracy of the conducted modeling.

Furthermore, Table 8 confirms a comparison between the achieved outcomes of the current study and the reported experimental results by Huang et al. [47]. It is brilliantly clear that relying on the obtained results by changing in T_g and T_c^*, the modeling results of the present work are in good accordance with the related results in Ref. [47].

Parametric study

In this section, the acquired results from the mathematical modeling and optimization of the offered energy system are reported.

To explore the consequences of design parameters on the offered systems' operation, a parametric study is carried out. Six critical parameters, namely: Steam to carbon molar ratio (S_c), Carbon dioxide to methane molar ratio (C_m), Reactor pressure (P_{Reac}), Reactor temperature (T_{Reac}), Evaporator temperature (T_{EVA}), and Environmental temperature (T_0) have been deemed as major design variables. Additionally, six operation parameters, namely: energy and exergy efficiencies, TCOP, net power, cooling capacity, and hydrogen rate are regarded as the objectives.

The effect of the carbon dioxide to methane molar ratio (C_m) on the performance of the system

As can be seen in Fig. 3, an increment in C_m leads to an increase in the biogas flow rate and results in an increment in the rate of hydrogen production, but on the other hand, according to the water shift equation, more hydrogen is consumed. Based on the discussion in Ref. [23], the growth of hydrogen consumption is higher than the production of hydrogen, and as a result, the hydrogen production trend is declining. So for C_m at 0.1, the rate of generated hydrogen is 723.7 kg/h. On the other hand, the biogas flow rate increases by increasing the carbon dioxide to methane molar ratio, and therefore more heat is transferred to the subsystems, and the net power and cooling power in C_m at 0.7 are maximized. It should be noted that the effect of hydrogen production is greater than cooling and net power production, and therefore energy and exergy efficiencies will have a similar trend as the

Table 8 – Ejector validation with experimental data [47].

T_g	T_c^*	μ			A_{11}/A_t		
		Experiment	Present study	Error (%)	Experiment	Present study	Error (%)
95	31.3	0.4377	0.39	10.90	10.64	10.34	2.82
95	33.0	0.3937	0.35	11.1	9.83	9.61	2.24
95	33.6	0.3457	0.34	1.64	9.41	9.37	0.43
95	34.2	0.3505	0.33	5.85	9.17	9.17	0
95	36.3	0.2814	0.29	3.05	8.28	8.39	1.32
95	37.1	0.2902	0.28	3.51	8.25	8.13	1.45
95	38.8	0.2273	0.24	5.59	7.26	7.59	4.54
95	38.6	0.2552	0.25	2.04	7.73	7.63	1.29
95	41.0	0.2043	0.21	2.80	6.77	6.94	2.51
95	42.1	0.1859	0.19	2.20	6.44	6.66	3.41
90	31.5	0.4446	0.48	7.96	9.41	9.02	4.14
90	33.8	0.3488	0.33	5.39	8.28	8.20	0.97
90	36.7	0.3040	0.28	7.89	7.73	7.28	5.82
90	37.5	0.2718	0.26	4.34	6.99	7.03	0.57
90	38.9	0.2246	0.23	2.40	6.44	6.64	3.11

Please cite this article as: He J et al., Multi-objective optimization and exergoeconomic analysis of a multi-generation system based on biogas-steam reforming, International Journal of Hydrogen Energy, https://doi.org/10.1016/j.ijhydene.2022.12.093

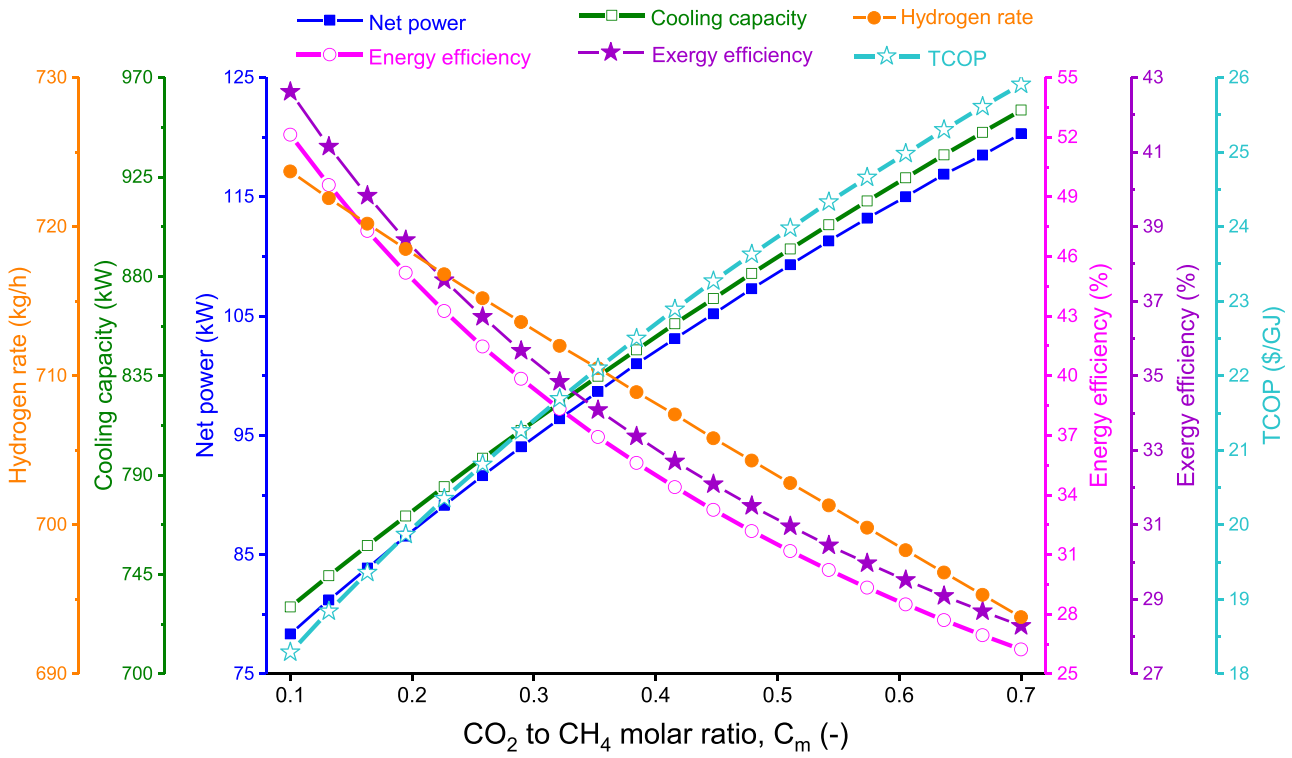

Fig. 3 – The effect of the carbon dioxide to methane molar ratio (C_m) on the thermodynamic efficiencies, TCOP, net power, cooling capacity, and hydrogen rates.

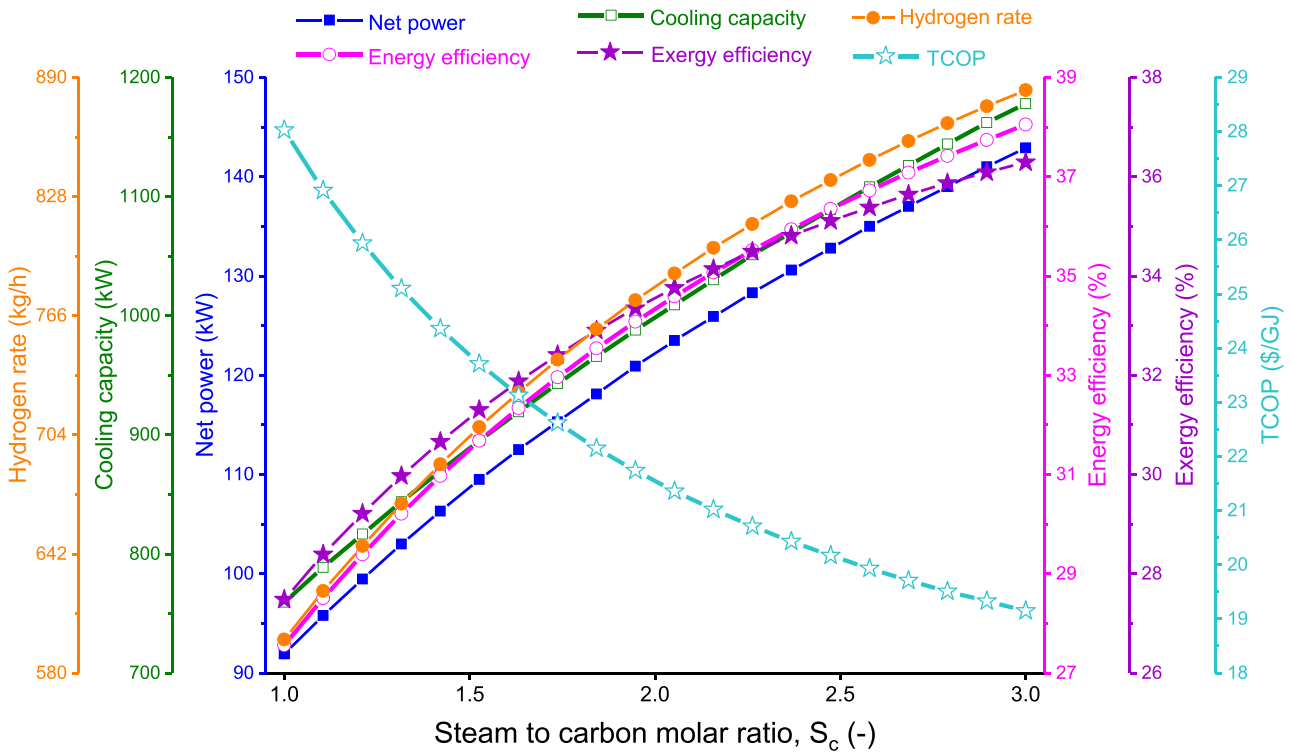

Fig. 4 – The effect of the steam-to-carbon molar ratio (S_c) on the thermodynamic efficiencies, TCOP, net power, cooling capacity, and hydrogen rates.

Please cite this article as: He J et al., Multi-objective optimization and exergoeconomic analysis of a multi-generation system based on biogas-steam reforming, International Journal of Hydrogen Energy, https://doi.org/10.1016/j.ijhydene.2022.12.093

rate of hydrogen production trend. Compared to other selected variables in the parametric study, most changes in energy and exergy efficiencies occur with changes in C_m. The trend of TCOP is similar to cooling and net power trends.

The effect of the steam-to-carbon molar ratio (S_c) on the performance of the system

According to Fig. 4, the improvement in S_c from 1 to 3, leads to more hydrogen production to balance the chemical reaction. In other words, the biogas flow rate is constant but the water vapor flow rate has increased, which has led to an increase in the rate of hydrogen production. On the other hand, the total flow through the reactor and vapor generators also has an increasing trend, which means more heat is injected into the subsystems. As a result, all three products have an upward trend with increasing S_c. Due to the above-mentioned reasons and the existing relationships for energy and exergy efficiencies, the growth of production has led to an increase in thermodynamic efficiencies. By increasing S_C, system costs are increasing, but the growth of production is significant, which reduces the TCOP. As a result, when S_c is at 3, TCOP has the lowest value at 19.15 $/GJ.

The effect of the reactor pressure (P_{Reac}) on the performance of the system

Referring to Fig. 5, growing the reactor pressure has no effect on the flow rates through the reactor. In other words, with increasing reactor pressure, rates of the biogas flow, water vapor flow, and exhaust gas flow do not change, but the hydrogen in the exhaust gas decreases. When the fraction of hydrogen decreases in the outlet gas, can be expected to see a decrement in enthalpy deference on both sides of vapor generators. As a result, the amount of heat injection into the subsystems experiences a decrement. On the other hand, the decrease in heat injected into the subsystems by increasing the reactor pressure leads to a decrease in power and cooling production. According to the above-mentioned reasons and the existing relationships for energy and exergy efficiencies, decrement in the amounts of the products by increasing reactor pressure results in a decrease in thermodynamic efficiencies. At a reactor pressure of 1 bar, energy and exergy efficiencies are 33.13% and 33.11%, sequentially. As the reactor pressure increases, system costs decrease, but the decrease in production is dominant, which increases the TCOP.

The effect of the reactor temperature (T_{Reac}) on the performance of the system

As the reactor temperature rises in Fig. 6, the rates of hydrogen production, power, and cooling capacity first increase and then decrease. In other words, the outputs of the system have one maximum point. Similar to the rational reason that has been expressed in Ref. [23], the reason for the improvement in hydrogen production rate with extending reactor temperature is the change in equilibrium towards the products. The maximum hydrogen production rate occurs at a reactor temperature of 1108 K, which is equal to 803.8 kg/h. The heat injected into the subsystems also has a maximum point, which leads to a maximum production point of net power and cooling capacity at a temperature of 1082 K, which are equal to 114.2 kW and 934.8 kW, sequentially. According to the earlier

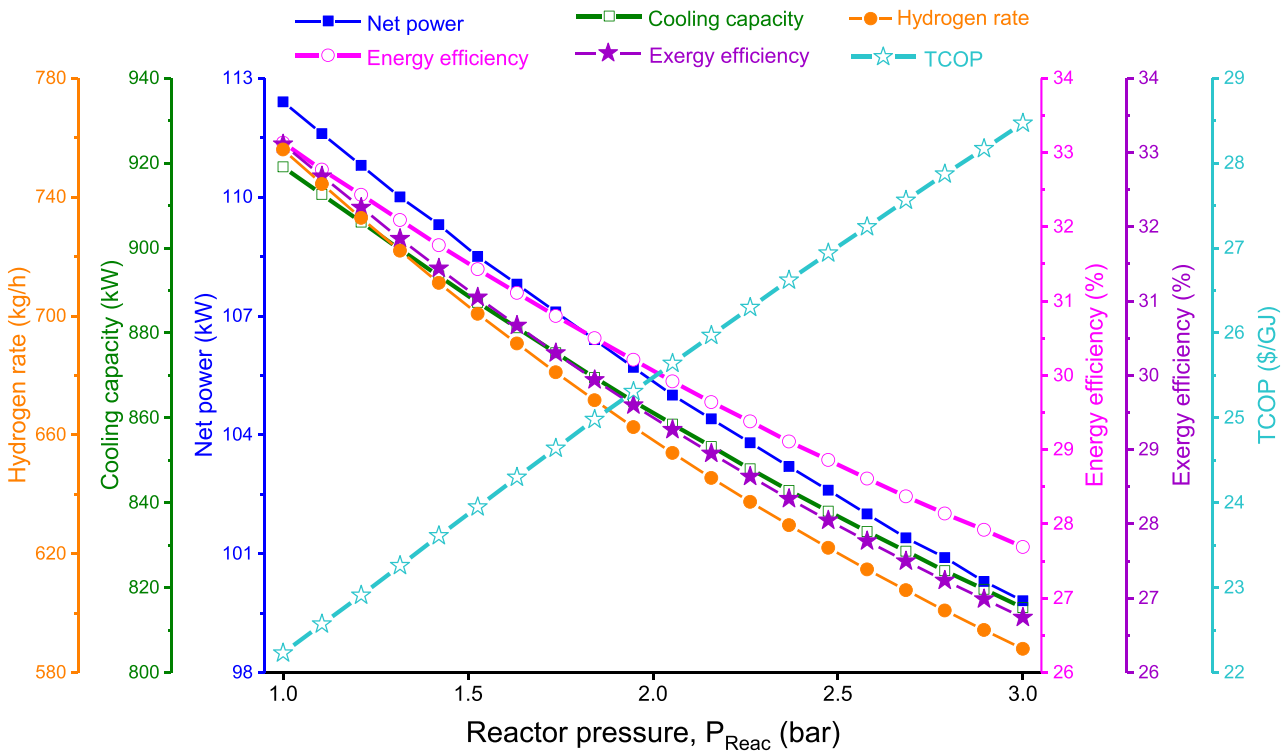

Fig. 5 – The effect of the reactor pressure (P_{Reac}) on the thermodynamic efficiencies, TCOP, net power, cooling capacity, and hydrogen rates.

Please cite this article as: He J et al., Multi-objective optimization and exergoeconomic analysis of a multi-generation system based on biogas-steam reforming, International Journal of Hydrogen Energy, https://doi.org/10.1016/j.ijhydene.2022.12.093

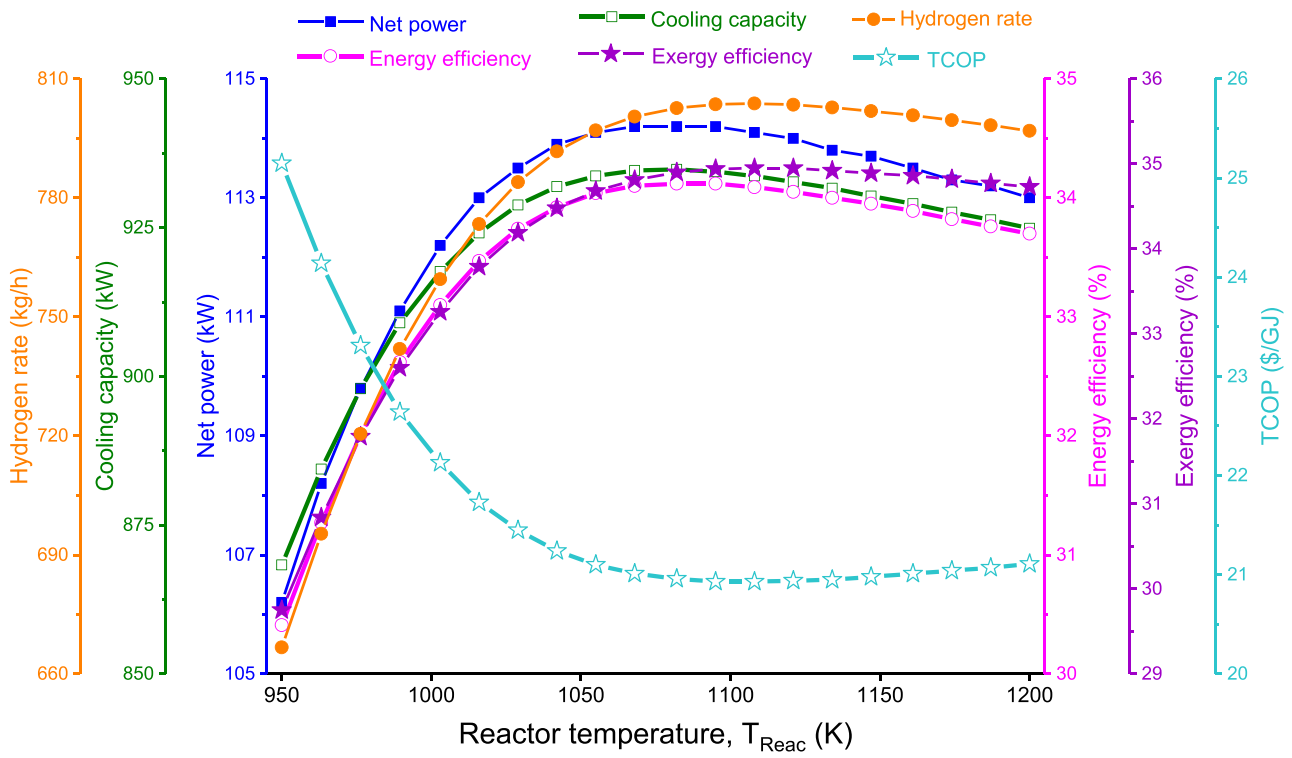

Fig. 6 – The effect of the reactor temperature (T_{Reac}) on the thermodynamic efficiencies, TCOP, net power, cooling capacity, and hydrogen rates.

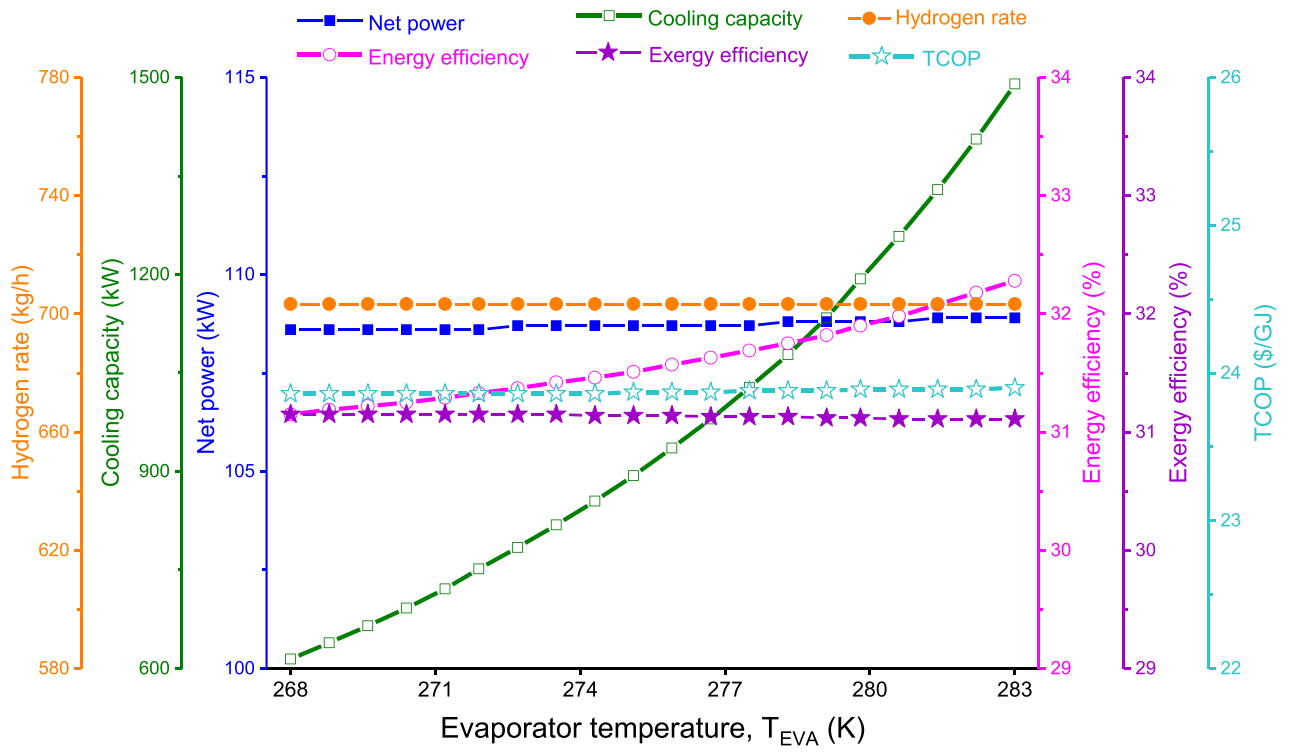

Fig. 7 – The effect of the evaporator temperature (T_{EVA}) on the thermodynamic efficiencies, TCOP, net power, cooling capacity, and hydrogen rates.

Please cite this article as: He J et al., Multi-objective optimization and exergoeconomic analysis of a multi-generation system based on biogas-steam reforming, International Journal of Hydrogen Energy, https://doi.org/10.1016/j.ijhydene.2022.12.093

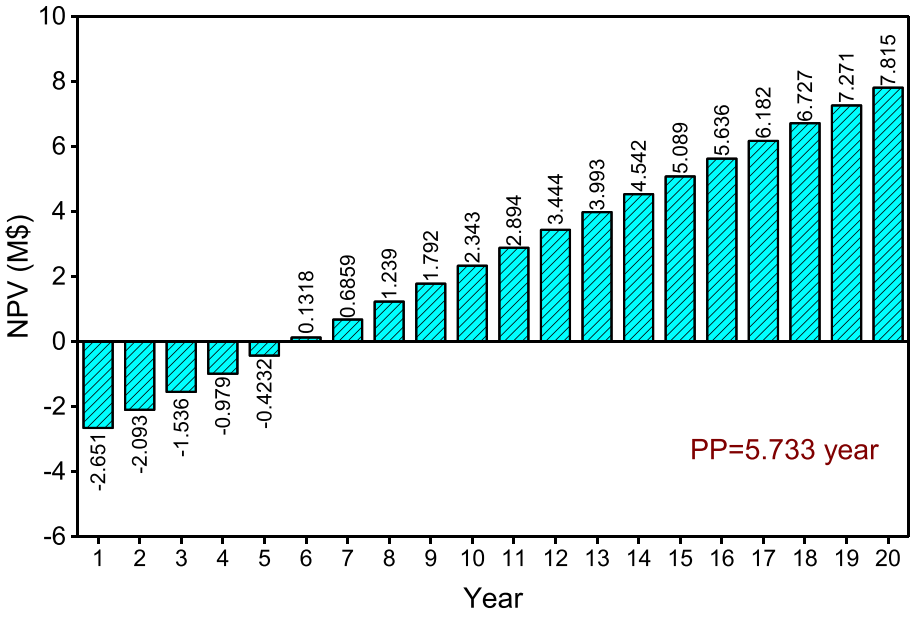

Fig. 8 – The impact of the changing life of the system on the NPV.

reasons and the existing relationships for energy and exergy efficiencies, at the reactor temperature of 1095 K, the energy efficiency is maximized and at the reactor temperature of 1108 K, the exergy efficiency is maximized, which both are equal to 34.12% and 34.95%, individually. The TCOP, according to the production process of the system has an optimal point (minimum), therefore, at a reactor temperature of 1108 K, TCOP has its lowest value, which is equal to 20.93 $/GJ.

The effect of the evaporator temperature (T_{EVA}) on the performance of the system

Relying on Fig. 7, the evaporator temperature variation does not affect the hydrogen production. Obviously, increasing the evaporator temperature leads to more cooling products, and therefore at the evaporator temperature of 283 K, the system is capable of producing 1490 kW of cooling, which shows a 142.5% increase compared to the evaporator temperature of 268 K. It should be noted that the power generation increases slightly with rising evaporator temperature, from 108.6 kW at 268 K to 189.9 kW at 283 K. Enhancing the production of power and cooling by rising the evaporator temperature, leads to an increment in energy efficiency from 31.15% to 32.28%. However, the exergy efficiency has a decreasing trend and at the evaporator temperature of 268 K, it has its maximum value of 31.15%. More cooling production results in a slight increase in TCOP which is 23.9 $/GJ at 283 K.

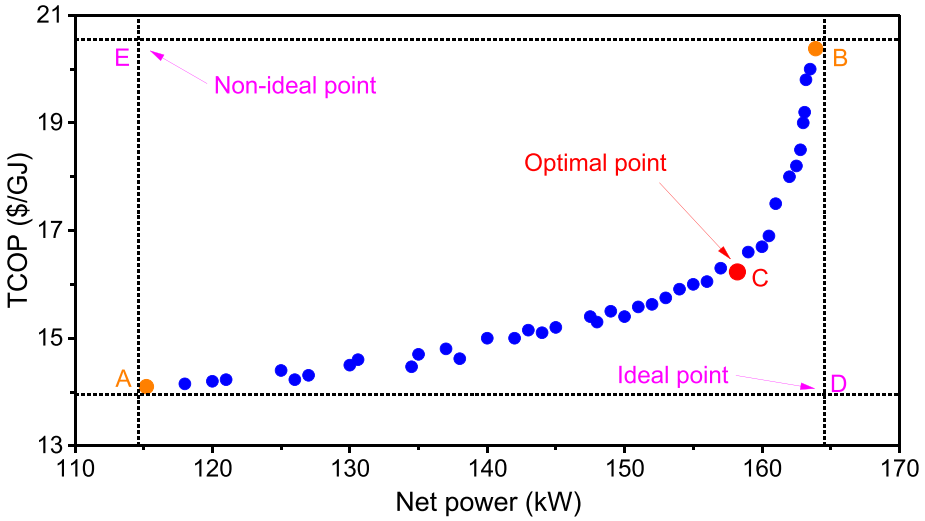

Fig. 9 – Pareto front and optimization solution points.

Please cite this article as: He J et al., Multi-objective optimization and exergoeconomic analysis of a multi-generation system based on biogas-steam reforming, International Journal of Hydrogen Energy, https://doi.org/10.1016/j.ijhydene.2022.12.093

Table 9 – Main outcomes of the proposed system.

Parameter	Two objective optimization			Base case
	A (lowest TCOP)	B (Highest $\dot{W}_{net}$)	C (Optimal point)	
$\dot{W}_{TUR1}$ (kW)	106.6	149.1	142.7	96.65
$\dot{W}_{TUR2}$ (kW)	22.29	25.88	24.95	18.68
$\dot{W}_{TUR3}$ (kW)	86.78	102.2	98.57	86.85
$\dot{W}_{TEG1}$ (kW)	10.32	16.83	16.22	12.6
$\dot{W}_{TEG2}$ (kW)	1.164	1.626	1.583	1.944
$\dot{W}_{PU1}$ (kW)	2.901	3.636	3.51	2.502
$\dot{W}_{PU2}$ (kW)	1.655	1.829	1.763	1.354
$\dot{W}_{PU3}$ (kW)	22.39	26.36	24.41	19.75
$\dot{W}_{CP1}$ (kW)	20.63	24.05	23.07	17.32
$\dot{W}_{CP2}$ (kW)	64.39	75.79	73.06	67.11
$\dot{W}_{net}$ (kW)	115.2	163.9	158.21	108.7
$\dot{Q}_{EVA1}$ (kW)	111.9	130.5	125.82	125.1
$\dot{Q}_{EVA2}$ (kW)	23.65	27.84	26.72	160.3
$\dot{Q}_{EVA3}$ (kW)	325.9	383.7	369.2	603.3
$\dot{Q}_{EVA}$ (kW)	461.5	542	521.74	888.7
$\dot{m}_{14}$ (kg /h)	953.4	888.5	930.95	703.3
η_{en} (%)	60.7	31.7	42.1	31.51
η_{ex} (%)	49.94	33.82	37.9	31.14
$\dot{E}x_D$ (kW)	10,420	24,995	19,637	13,622
TCOP ($/GJ)	14.1	20.38	16.23	23.87
NPV (M$)	5.866	6.524	6.035	7.815
PP (year)	9.89	8.69	9.43	5.733

The impact of the lifetime of the system on the NPV

NPV is an economic analysis to calculate the return time of initial investment and the final profit during the life of the offered system. According to Fig. 8, it is clear that after 5.733 years, the initial capital returns, and in the 20th year, the system has a profitability of about 7.815 million dollars. This figure shows the NPV values for the first to twentieth year separately.

Solution of the optimization problem

In order to improve the performance of the proposed energy system, the single optimal design, and multi-objective optimal design methods are applied. Fig. 9 shows the Pareto front. Points A and B show the single-optimization based on the lowest TCOP and the highest net power production, individually. By drawing a line perpendicular to these points, point D is an ideal point that is almost impossible to achieve. Point C is the optimal point for the proposed system from a multi-objective optimization point of view. Minimum TCOP and maximum generated power have occurred in Point C simulants at the same time.

Moreover, Table 9 shows a comprehensive identification of system operation optimized by single-objective optimization and multi-objective optimization methods. Furthermore, the mentioned table reviews key variables and objective functions and their changes after the optimization process in different optimization techniques. Relying on Table 9, in the base case, energetic and exergetic efficiencies of the offered system are 31.51%, and 31.14%, sequentially. While the mentioned values improve and reach 42.1% and 37.9% after multi-objective optimization. Also, the rate of generated hydrogen improves from 703.3 kg/h in the base case to 930.95 kg/h in the multi-objective optimization case in Point C. Moreover, from the acquired data, it is concluded that considering the minimization of TCOP as a main and sole target in the optimization process, the TCOP reaches its lowest value (14.1$/GJ) in Point A. Also, in Point B, the net power produced is at its maximum amount of 163.9 kW, while in the base case is 108.7 kW.

Conclusions

A new multi-generation integrated energy system for hydrogen, power, and cooling production powered by biogas reforming is developed and assessed from energy, exergy, and thermoeconomic aspects. To improve the rate of hydrogen generation, the biogas-steam reforming and the purification process are integrated into the offered multi-generation configuration. This cycle has a high ability to integrate with cooling cycles and also has higher exergy efficiency than the Rankine organic cycle under the same working conditions. Also, R236fa refrigerant is employed in subsystems due to its environmental friendliness and also producing more cooling load than other refrigerants.

Moreover, to appraise the importance of input design variables on the performance criteria of the offered system, a comprehensive parametric study is conducted and debated in detail. Also, two different optimization modes (single and multi-objective) are applied to detect optimum working conditions and find the most optimal results. Some of the remarkable concluding points of the current work are stated below:

- The energy and the exergy efficiencies plus TCOP of the multi-generation system have been calculated at 31.51%, 31.14%, and 23.87 $/GJ, sequentially. Also, the net power output, the cooling load, and the hydrogen production rate of the multi-generation system are estimated at 108.7 kW, 888.7 kW, and 703.3 kg/h.
- After 5.733 years, the initial capital returns, and in the 20th year, the system has a profitability of about 7.815 million dollars.
- From the optimization results, the TCOP stands at its smallest value (14.1 $/GJ) after an individual single optimization method, and the net power touches the highest amounts (163.9 kW) after an individual single optimization method. Through multi-objective optimization, optimal operation points of the system are obtained at a TCOP of 16.23 S/GJ and a net power of 158.21 kW.

Declaration of competing interest

The authors declare that they have no known competing financial interests or personal relationships that could have appeared to influence the work reported in this paper.

Please cite this article as: He J et al., Multi-objective optimization and exergoeconomic analysis of a multi-generation system based on biogas-steam reforming, International Journal of Hydrogen Energy, https://doi.org/10.1016/j.ijhydene.2022.12.093

REFERENCES

[1] Sani MM, et al. Optimal energy hub development to supply heating, cooling, electricity and freshwater for a coastal urban area taking into account economic and environmental factors. Energy 2022;238:121743.
[2] Hashemian N, Noorpoor A, Heidarnejad P. Thermodynamic diagnosis of a novel solar-biomass based multi-generation system including potable water and hydrogen production. Energy Equip Syst 2019;7(1):81–98.
[3] Cao Y, et al. A novel multi-objective spiral optimization algorithm for an innovative solar/biomass-based multi-generation energy system: 3E analyses, and optimization algorithms comparison. Energy Convers Manag 2020;219:112961.
[4] Hasanzadeh A, et al. Stand-alone gas turbine and hybrid MCFC and SOFC-gas turbine systems: comparative life cycle cost, environmental, and energy assessments. Energy Rep 2021;7:4659–80.
[5] Noorpoor A, et al. A thermodynamic model for exergetic performance and optimization of a solar and biomass-fuelled multigeneration system. Energy Equip Syst 2016;4(2):281–9.
[6] Heïdarnejad P. Exergy based optimization of a biomass and solar fuelled CCHP hybrid seawater desalination plant. J Therm Eng 2017;3(1):1034–43.
[7] Ghaebi H, et al. Energy, exergy, economic and environmental (4E) analysis of using city gate station (CGS) heater waste for power and hydrogen production: a comparative study. Int J Hydrogen Energy 2018;43(3):1855–74.
[8] Akhoondi A, et al. Recent advances in hydrogen production using MXenes-based metal sulfide photocatalysts. Synthesis and Sintering 2022;2(1):37–54.
[9] Ghaebi H, et al. Energy, exergy and thermoeconomic analysis of the novel combined cycle of solid oxide fuel cell (SOFC) and biogas steam reforming (BSR) for cogeneration power and hydrogen. Amirkabir Journal of Mechanical Engineering 2022;54(1). 10-10.
[10] Xu Y-P, et al. Optimization of a biomass-driven Rankine cycle integrated with multi-effect desalination, and solid oxide electrolyzer for power, hydrogen, and freshwater production. Desalination 2022;525:115486.
[11] Gnaifaid H, Ozcan H. Development and multiobjective optimization of an integrated flash-binary geothermal power plant with reverse osmosis desalination and absorption refrigeration for multi-generation. Geothermics 2021;89:101949.
[12] Li J, Zoghi M, Zhao L. Thermo-economic assessment and optimization of a geothermal-driven tri-generation system for power, cooling, and hydrogen production. Energy 2022;244:123151.
[13] You D, et al. Design and analysis of a solar energy driven tri-generation plant for power, heating, and refrigeration. J Energy Resour Technol 2022;144(8).
[14] Colakoglu M, Durmayaz A. Energy, exergy and economic analyses and multiobjective optimization of a novel solar multi-generation system for production of green hydrogen and other utilities. Int J Hydrogen Energy 2022;47(45):19446–62.
[15] Cao Y, et al. Hydrogen production using solar energy and injection into a solid oxide fuel cell for CO2 emission reduction; Thermoeconomic assessment and tri-objective optimization. Sustain Energy Technol Assessments 2022;50:101767.
[16] Hashemian N, Noorpoor A. A geothermal-biomass powered multi-generation plant with freshwater and hydrogen generation options: thermo-economic-environmental appraisals and multi-criteria optimization. Renew Energy 2022;198:254–66.
[17] Ghaebi H, et al. Thermodynamic modeling and optimization of a combined biogas steam reforming system and organic Rankine cycle for coproduction of power and hydrogen. Renew Energy 2019;130:87–102.
[18] Situmorang YA, et al. A small-scale power generation system based on biomass direct chemical looping process with organic rankine cycle. Chemical Engineering and Processing-Process Intensification 2021;163:108361.
[19] Gholizadeh T, Vajdi M, Mohammadkhani F. Thermodynamic and thermoeconomic analysis of basic and modified power generation systems fueled by biogas. Energy Convers Manag 2019;181:463–75.
[20] Minutillo M, Perna A, Sorce A. Green hydrogen production plants via biogas steam and autothermal reforming processes: energy and exergy analyses. Appl Energy 2020;277:115452.
[21] Klein S. Engineering equation solver (EES) V9. Madison, USA: F-chart software; 2015.
[22] Azariyan H, Vajdi M, Takleh HR. Assessment of a high-performance geothermal-based multigeneration system for production of power, cooling, and hydrogen: thermodynamic and exergoeconomic evaluation. Energy Convers Manag 2021;236:113970.
[23] Rostamzadeh H, et al. A novel multigeneration system driven by a hybrid biogas-geothermal heat source, Part I: thermodynamic modeling. Energy Convers Manag 2018;177:535–62.
[24] Takleh HR, Zare V. Employing thermoelectric generator and booster compressor for performance improvement of a geothermal driven combined power and ejector-refrigeration cycle. Energy Convers Manag 2019;186:120–30.
[25] Mosaffa A, Zareei A. Proposal and thermoeconomic analysis of geothermal flash binary power plants utilizing different types of organic flash cycle. Geothermics 2018;72:47–63.
[26] Takleh HR, Zare V. Proposal and thermoeconomic evaluation with reliability considerations of geothermal driven trigeneration systems with independent operations for summer and winter. Int J Refrig 2021;127:34–46.
[27] Wang Y, et al. A novel cooling and power cycle based on the absorption power cycle and booster-assisted ejector refrigeration cycle driven by a low-grade heat source: energy, exergy and exergoeconomic analysis, vol. 204. Energy Conversion and Management; 2020, 112321.
[28] Cao Y, et al. Seasonal design and multi-objective optimization of a novel biogas-fueled cogeneration application. Int J Hydrogen Energy 2021;46(42):21822–43.
[29] Noorpoor A, Hashemian N, Heidarnejad P. Thermodynamic assessment of an integrated solar-biomass system for quadruple generation purposes. J Sol Energy Res 2016;1(1):53–8.
[30] Ghaebi H, et al. Energy, exergy and exergoeconomic analysis of a cogeneration system for power and hydrogen production purpose based on TRR method and using low grade geothermal source. Geothermics 2018;71:132–45.
[31] Hashemian N, Noorpoor A, Amidpour M. A biomass assisted solar-based multi-generation plant with hydrogen and freshwater production: sustainability, advanced exergy and advanced exergo-economic assessments. In: Synergy development in renewables assisted multi-carrier systems. Springer; 2022. p. 107–25.
[32] Feili M, et al. Hydrogen extraction from a new integrated trigeneration system working with zeotropic mixture, using waste heat of a marine diesel engine. Int J Hydrogen Energy 2020;45(41):21969–94.
[33] Ghaebi H, et al. Proposal and assessment of a novel geothermal combined cooling and power cycle based on

Please cite this article as: He J et al., Multi-objective optimization and exergoeconomic analysis of a multi-generation system based on biogas-steam reforming, International Journal of Hydrogen Energy, https://doi.org/10.1016/j.ijhydene.2022.12.093

Kalina and ejector refrigeration cycles. Appl Therm Eng 2018;130:767–81.
[34] Ghaebi H, et al. Thermodynamic and thermoeconomic analysis and optimization of a novel combined cooling and power (CCP) cycle by integrating of ejector refrigeration and Kalina cycles. Energy 2017;139:262–76.
[35] Hashemian N, Noorpoor A. Assessment and multi-criteria optimization of a solar and biomass-based multi-generation system: thermodynamic, exergoeconomic and exergoenvironmental aspects. Energy Convers Manag 2019;195:788–97.
[36] Cao Y, et al. Multi-objective bat optimization for a biomass gasifier integrated energy system based on 4E analyses. Appl Therm Eng 2021;196:117339.
[37] Rostamzadeh H, et al. A novel multigeneration system driven by a hybrid biogas-geothermal heat source, Part II: multi-criteria optimization. Energy Convers Manag 2019;180:859–88.
[38] Takleh HR, Zare V. Performance improvement of ejector expansion refrigeration cycles employing a booster compressor using different refrigerants: thermodynamic analysis and optimization. Int J Refrig 2019;101:56–70.
[39] Cao Y, et al. Effect of working fluids in a novel geothermal-based integration of organic-flash and power/cooling generation cycles with hydrogen and freshwater production units. Int J Hydrogen Energy 2021;46(56):28370–86.
[40] Parikhani T, et al. Thermodynamic and thermoeconomic analysis of a novel ammonia-water mixture combined cooling, heating, and power (CCHP) cycle. Renew Energy 2020;145:1158–75.
[41] Noorpoor A, Hamedi D, Hashemian N. Optimization of parabolic trough solar collectors integrated with two stage Rankine cycle. J Sol Energy Res 2017;2(2):61–6.
[42] Cao Y, et al. Development, assessment and comparison of three high-temperature geothermal-driven configurations for power and hydrogen generation: energy, exergy thermoeconomic and optimization. Int J Hydrogen Energy 2020;45(58):34163–84.
[43] Heidarnejad P, Hashemian N, Noorpoor AR. Multi objective exergy based optimization of a solar micro CHP system based on organic rankine cycle. J Sol Energy Res 2017;2(2):41–7.
[44] Lee HY, Park SH, Kim KH. Comparative analysis of thermodynamic performance and optimization of organic flash cycle (OFC) and organic Rankine cycle (ORC). Appl Therm Eng 2016;100:680–90.
[45] Wegeng R, Diver R, Humble P. Second law analysis of a solar methane reforming system. Energy Proc 2014;49:1248–58.
[46] Madhawa Hettiarachchi H, et al. The performance of the Kalina cycle system 11 (KCS-11) with low-temperature heat sources. 2007.
[47] Huang B, et al. A 1-D analysis of ejector performance. Int J Refrig 1999;22(5):354–64.

Please cite this article as: He J et al., Multi-objective optimization and exergoeconomic analysis of a multi-generation system based on biogas-steam reforming, International Journal of Hydrogen Energy, https://doi.org/10.1016/j.ijhydene.2022.12.093